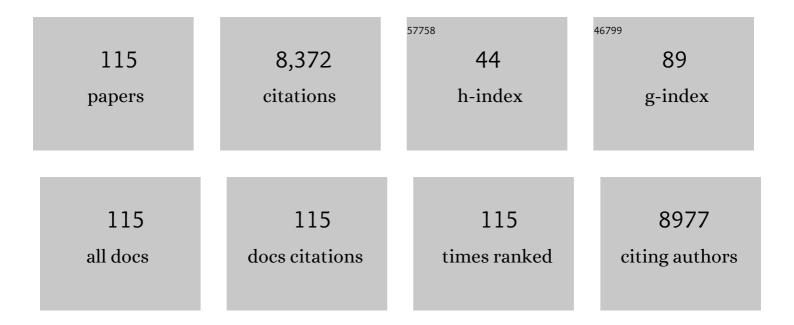
## Mark A Horsfield

List of Publications by Year in descending order

Source: https://exaly.com/author-pdf/2785292/publications.pdf Version: 2024-02-01



#	Article	IF	CITATIONS
1	Dynamic Contrast-Enhanced Magnetic Resonance Imaging As a Biomarker for the Pharmacological Response of PTK787/ZK 222584, an Inhibitor of the Vascular Endothelial Growth Factor Receptor Tyrosine Kinases, in Patients With Advanced Colorectal Cancer and Liver Metastases: Results From Two Phase I Studies. Journal of Clinical Oncology, 2003, 21, 3955-3964.	1.6	648
2	Non-invasive assessment of axonal fiber connectivity in the human brain via diffusion tensor MRI. Magnetic Resonance in Medicine, 1999, 42, 37-41.	3.0	544
3	Applications of diffusion-weighted and diffusion tensor MRI to white matter diseases - a review. NMR in Biomedicine, 2002, 15, 570-577.	2.8	435
4	Magnetization transfer changes in the normal appering white matter precede the appearance of enhancing lesions in patients with multiple sclerosis. Annals of Neurology, 1998, 43, 809-814.	5.3	356
5	Characterization of White Matter Damage in Ischemic Leukoaraiosis with Diffusion Tensor MRI. Stroke, 1999, 30, 393-397.	2.0	302
6	MRI in multiple sclerosis: current status and future prospects. Lancet Neurology, The, 2008, 7, 615-625.	10.2	295
7	Rapid semi-automatic segmentation of the spinal cord from magnetic resonance images: Application in multiple sclerosis. NeuroImage, 2010, 50, 446-455.	4.2	234
8	Phase I Study of the Safety, Tolerability, Pharmacokinetics, and Pharmacodynamics of PTK787/ZK 222584 Administered Twice Daily in Patients With Advanced Cancer. Journal of Clinical Oncology, 2005, 23, 4162-4171.	1.6	230
9	Age effects on diffusion tensor magnetic resonance imaging tractography measures of frontal cortex connections in schizophrenia. Human Brain Mapping, 2006, 27, 230-238.	3.6	224
10	Spatial Normalization and Averaging of Diffusion Tensor MRI Data Sets. NeuroImage, 2002, 17, 592-617.	4.2	208
11	A myocardial perfusion reserve index in humans using first-pass contrast-enhanced magnetic resonance imaging. Journal of the American College of Cardiology, 1999, 33, 1386-1394.	2.8	195
12	Brain MRI atrophy quantification in MS. Neurology, 2017, 88, 403-413.	1.1	188
13	A method for obtaining tract-specific diffusion tensor MRI measurements in the presence of disease: application to patients with clinically isolated syndromes suggestive of multiple sclerosis. NeuroImage, 2005, 26, 258-265.	4.2	182
14	Apparent diffusion coefficients in benign and secondary progressive multiple sclerosis by nuclear magnetic resonance. Magnetic Resonance in Medicine, 1996, 36, 393-400.	3.0	176
15	Gray matter damage predicts the accumulation of disability 13 years later in MS. Neurology, 2013, 81, 1759-1767.	1.1	174
16	lsotropic resolution diffusion tensor imaging with whole brain acquisition in a clinically acceptable time. Human Brain Mapping, 2002, 15, 216-230.	3.6	172
17	Guidelines for using quantitative measures of brain magnetic resonance imaging abnormalities in monitoring the treatment of multiple sclerosis. Annals of Neurology, 1998, 43, 499-506.	5.3	152
18	Brain network connectivity assessed using graph theory in frontotemporal dementia. Neurology, 2013, 81, 134-143.	1.1	139

#	Article	IF	CITATIONS
19	lmaging vascular function for early stage clinical trials using dynamic contrast-enhanced magnetic resonance imaging. European Radiology, 2012, 22, 1451-1464.	4.5	138
20	T1/T2 Ratio and Frequency Dependence of NMR Relaxation in Porous Sedimentary Rocks. Journal of Colloid and Interface Science, 1993, 158, 195-198.	9.4	134
21	Mean diffusivity and fractional anisotropy histogram analysis of the cervical cord in MS patients. NeuroImage, 2005, 26, 822-828.	4.2	123
22	Magnetic Resonance Techniques in Multiple Sclerosis. Archives of Neurology, 2011, 68, 1514.	4.5	120
23	Visualization of cranial nerves I-XII: value of 3D CISS and T2-weighted FSE sequences. European Radiology, 2000, 10, 1061-1067.	4.5	116
24	Cortical Abnormalities in Patients with Migraine: A Surface-based Analysis. Radiology, 2013, 268, 170-180.	7.3	105
25	Mapping eddy current induced fields for the correction of diffusion-weighted echo planar images. Magnetic Resonance Imaging, 1999, 17, 1335-1345.	1.8	103
26	Recommendations to improve imaging and analysis of brain lesion load and atrophy in longitudinal studies of multiple sclerosis. Journal of Neurology, 2013, 260, 2458-2471.	3.6	96
27	Spatial normalization and averaging of diffusion tensor MRI data sets. NeuroImage, 2002, 17, 592-617.	4.2	96
28	Intercenter differences in diffusion tensor MRI acquisition. Journal of Magnetic Resonance Imaging, 2010, 31, 1458-1468.	3.4	81
29	3ÂT MRI relaxometry detects T2 prolongation in the cerebral normal-appearing white matter in multiple sclerosis. NeuroImage, 2009, 46, 633-641.	4.2	72
30	Magnetization Transfer Imaging in Multiple Sclerosis. Journal of Neuroimaging, 2005, 15, 58S-67S.	2.0	69
31	Myocardial T1 and extracellular volume fraction measurement in asymptomatic patients with aortic stenosis: reproducibility and comparison with age-matched controls. European Heart Journal Cardiovascular Imaging, 2015, 16, 763-770.	1.2	67
32	Sensitivity-encoded diffusion tensor MR imaging of the cervical cord. American Journal of Neuroradiology, 2003, 24, 1254-6.	2.4	67
33	Guidelines for using quantitative magnetization transfer magnetic resonance imaging for monitoring treatment of multiple sclerosis. Journal of Magnetic Resonance Imaging, 2003, 17, 389-397.	3.4	66
34	Biomarkers for assessment of pharmacologic activity for a vascular endothelial growth factor (VEGF) receptor inhibitor, PTK787/ZK 222584 (PTK/ZK): translation of biological activity in a mouse melanoma metastasis model to phase I studies in patients with advanced colorectal cancer with liver metastases. Cancer Chemotherapy and Pharmacology, 2006, 57, 761-771.	2.3	66
35	A 6â€year clinical and MRI followâ€up study of patients with relapsing–remitting multiple sclerosis treated with Interferonâ€beta. European Journal of Neurology, 2002, 9, 645-655.	3.3	65
36	Intertechnique agreement and interstudy reproducibility of strain and diastolic strain rate at 1.5 and 3 tesla: A comparison of featureâ€ŧracking and tagging in patients with aortic stenosis. Journal of Magnetic Resonance Imaging, 2015, 41, 1129-1137.	3.4	64

#	Article	IF	CITATIONS
37	Subclinical diastolic dysfunction in young adults with Type 2 diabetes mellitus: a multiparametric contrast-enhanced cardiovascular magnetic resonance pilot study assessing potential mechanisms. European Heart Journal Cardiovascular Imaging, 2014, 15, 1263-1269.	1.2	58
38	Cluster Analysis of Diffusion Tensor Magnetic Resonance Images in Human Head Injury. Neurosurgery, 2000, 47, 306-314.	1.1	57
39	Posterior brain damage and cognitive impairment in pediatric multiple sclerosis. Neurology, 2014, 82, 1314-1321.	1.1	56
40	A simple, reproducible method for monitoring the treatment of tumours using dynamic contrast-enhanced MR imaging. British Journal of Cancer, 2006, 94, 1420-1427.	6.4	55
41	The physical basis of diffusion-weighted MRI. Journal of the Neurological Sciences, 2001, 186, S11-S14.	0.6	54
42	Macroscopic and microscopic assessments of disease burden by MRI in multiple sclerosis: Relationship to clinical parameters. Journal of Magnetic Resonance Imaging, 1996, 6, 580-584.	3.4	50
43	Benign and secondary progressive multiple sclerosis: a preliminary quantitative MRI study. Journal of Neurology, 1994, 241, 246-251.	3.6	48
44	Whole-brain atrophy in multiple sclerosis measured by two segmentation processes from various MRI sequences. Journal of the Neurological Sciences, 2003, 216, 169-177.	0.6	47
45	Ultra-high-field MR imaging in multiple sclerosis. Journal of Neurology, Neurosurgery and Psychiatry, 2014, 85, 60-66.	1.9	47
46	Measurement of Whole-Brain and Gray Matter Atrophy in Multiple Sclerosis: Assessment with MR Imaging. Radiology, 2018, 288, 554-564.	7.3	47
47	Self-diffusion in CNS tissue by volume-selective proton NMR. Magnetic Resonance in Medicine, 1994, 31, 637-644.	3.0	42
48	Voxel-wise mapping of cervical cord damage in multiple sclerosis patients with different clinical phenotypes. Journal of Neurology, Neurosurgery and Psychiatry, 2013, 84, 35-41.	1.9	42
49	Regional Cervical Cord Atrophy and Disability in Multiple Sclerosis: A Voxel-based Analysis. Radiology, 2013, 266, 853-861.	7.3	42
50	A Diffusion Tensor Magnetic Resonance Imaging Study of Frontal Cortex Connections in Very-Late-Onset Schizophrenia-Like Psychosis. American Journal of Geriatric Psychiatry, 2005, 13, 1092-1099.	1.2	42
51	Intranetwork and internetwork functional connectivity abnormalities in pediatric multiple sclerosis. Human Brain Mapping, 2014, 35, 4180-4192.	3.6	40
52	Microstructural magnetic resonance imaging of cortical lesions in multiple sclerosis. Multiple Sclerosis Journal, 2013, 19, 418-426.	3.0	38
53	Spatial Normalization and Regional Assessment of Cord Atrophy: Voxel-Based Analysis of Cervical Cord 3D T1-Weighted Images. American Journal of Neuroradiology, 2012, 33, 2195-2200.	2.4	37
54	Does Stroke Subtype and Measurement Technique Influence Estimation of Cerebral Autoregulation in Acute Ischaemic Stroke?. Cerebrovascular Diseases, 2013, 35, 257-261.	1.7	35

#	Article	IF	CITATIONS
55	Size Distribution of Air Bubbles Entering the Brain during Cardiac Surgery. PLoS ONE, 2015, 10, e0122166.	2.5	35
56	Perioperative Cerebral Microbleeds After Adult Cardiac Surgery. Stroke, 2019, 50, 336-343.	2.0	34
57	Interhemispheric asymmetry of brain diffusivity in normal individuals: a diffusion-weighted MR imaging study. American Journal of Neuroradiology, 2005, 26, 1089-94.	2.4	34
58	DynamicT1Measurement Using Snapshot-FLASH MRI. Journal of Magnetic Resonance, 1997, 127, 65-72.	2.1	31
59	Dynamic Change of the Upper Airway during Inhalation via Aerosol Delivery Devices. Journal of Aerosol Medicine and Pulmonary Drug Delivery, 2004, 17, 325-334.	1.2	31
60	Impact of Perioperative Infarcts After Cardiac Surgery. Stroke, 2015, 46, 680-686.	2.0	31
61	Regional Differences in Dynamic Cerebral Autoregulation in the Healthy Brain Assessed by Magnetic Resonance Imaging. PLoS ONE, 2013, 8, e62588.	2.5	30
62	Associations of Sedentary Time with Fat Distribution in a High-Risk Population. Medicine and Science in Sports and Exercise, 2015, 47, 1727-1734.	0.4	30
63	Structural connectivity in multiple sclerosis and modeling of disconnection. Multiple Sclerosis Journal, 2020, 26, 220-232.	3.0	28
64	Assessing atrophy of the major white matter fiber bundles of the brain from diffusion tensor MRI data. Magnetic Resonance in Medicine, 2007, 58, 527-534.	3.0	27
65	Dynamic variations in the ultrasound greyscale median of carotid artery plaques. Cardiovascular Ultrasound, 2013, 11, 21.	1.6	27
66	Imaging Cortical Damage and Dysfunction in Multiple Sclerosis. JAMA Neurology, 2013, 70, 556.	9.0	27
67	Comparison of semi-automated methods to quantify infarct size and area at risk by cardiovascular magnetic resonance imaging at 1.5T and 3.0T field strengths. BMC Research Notes, 2015, 8, 52.	1.4	27
68	Contrast-Reduced Imaging of Tissue Concentration and Arterial Level (CRITICAL) for Assessment of Cerebral Hemodynamics in Acute Stroke by Magnetic Resonance. Investigative Radiology, 2000, 35, 401-411.	6.2	26
69	Nuclear magnetic resonance imaging of dairy products in two and three dimensions. International Dairy Journal, 1995, 5, 311-319.	3.0	25
70	A one year study of new lesions in multiple sclerosis using monthly gadolinium enhanced MRI: Correlations with changes of T2 and magnetization transfer lesion loads. Journal of the Neurological Sciences, 1998, 158, 203-208.	0.6	25
71	A Magnetization Transfer MRI Study of Deep Gray Matter Involvement in Multiple Sclerosis. Journal of Neuroimaging, 2006, 16, 302-310.	2.0	24
72	Dynamic cerebral autoregulation following acute ischaemic stroke: Comparison of transcranial Doppler and magnetic resonance imaging techniques. Journal of Cerebral Blood Flow and Metabolism, 2016, 36, 2194-2202.	4.3	24

#	Article	IF	CITATIONS
73	Depth Filtration of Clay in Rock Cores Observed by One-Dimensional 1H NMR Imaging. Journal of Colloid and Interface Science, 1993, 156, 253-255.	9.4	23
74	Protein-ligand interactions measured by 15N-filtered diffusion experiments. Journal of Biomolecular NMR, 1999, 13, 223-232.	2.8	23
75	ls Abdominal Fat Distribution Measured by Axial CT Imaging an Indicator of Complications and Mortality in Acute Pancreatitis?. Journal of Gastrointestinal Surgery, 2015, 19, 2126-2131.	1.7	22
76	The influence of clinical relapses and steroid therapy on the development of Gd-enhancing lesions: a longitudinal MRI study in relapsing-remitting multiple sclerosis patients. Acta Neurologica Scandinavica, 1997, 95, 201-207.	2.1	21
77	Algorithms for calculation of kinetic parameters from T1-weighted dynamic contrast-enhanced magnetic resonance imaging. Journal of Magnetic Resonance Imaging, 2004, 20, 723-729.	3.4	21
78	Quantitative assessment of carotid plaque surface irregularities and correlation to cerebrovascular symptoms. Cardiovascular Ultrasound, 2013, 11, 38.	1.6	21
79	T1- vs. T2-based MRI measures of spinal cord volume in healthy subjects and patients with multiple sclerosis. BMC Neurology, 2015, 15, 124.	1.8	21
80	True water and fat MR imaging with use of multiple-echo acquisition Radiology, 1989, 173, 249-253.	7.3	20
81	Incorporating Domain Knowledge Into the Fuzzy Connectedness Framework: Application to Brain Lesion Volume Estimation in Multiple Sclerosis. IEEE Transactions on Medical Imaging, 2007, 26, 1670-1680.	8.9	20
82	Measurement of Cerebral Blood Flow Responses to the Thigh Cuff Maneuver: A Comparison of TCD with a Novel MRI Method. Journal of Cerebral Blood Flow and Metabolism, 2011, 31, 1302-1310.	4.3	19
83	A longitudinal MRI study of cervical cord atrophy in multiple sclerosis. Journal of Neurology, 2015, 262, 1622-1628.	3.6	19
84	Quantitative Determination of Water and Lipid in Sunflower Oil and Water/Meat/Fat Emulsions by Nuclear Magnetic Resonance Imaging. Journal of Food Science, 1994, 59, 808-812.	3.1	18
85	A functional form for injected MRI Gd-chelate contrast agent concentration incorporating recirculation, extravasation and excretion. Physics in Medicine and Biology, 2009, 54, 2933-2949.	3.0	18
86	Using diffusion-weighted MRI in multicenter clinical trials for multiple sclerosis. Journal of the Neurological Sciences, 2001, 186, S51-S54.	0.6	17
87	Sedentary Time and MRIâ€Derived Measures of Adiposity in Active Versus Inactive Individuals. Obesity, 2018, 26, 29-36.	3.0	17
88	The role of imaging in the clinical development of antiangiogenic agents. Hematology/Oncology Clinics of North America, 2004, 18, 1183-1206.	2.2	16
89	A comparison of polyacrylamide gels and radiochromic film for source measurements in intravascular brachytherapy. British Journal of Radiology, 2003, 76, 824-831.	2.2	15
90	Control of gas phase nanoparticle shape and its effect on MRI relaxivity. Materials Research Express, 2015, 2, 035002.	1.6	15

#	Article	IF	CITATIONS
91	Characterisation of cardiomyopathy by cardiac and aortic magnetic resonance in patients new to hemodialysis. European Radiology, 2016, 26, 2749-2761.	4.5	15
92	Detection of Focal Longitudinal Changes in the Brain by Subtraction of MR Images. American Journal of Neuroradiology, 2017, 38, 923-927.	2.4	14
93	Optimization of a Breath-Hold Magnetic Resonance Gradient Echo Technique for the Detection of Interstitial Lung Disease. Investigative Radiology, 1995, 30, 730-737.	6.2	13
94	Aortic stiffness in aortic stenosis assessed by cardiovascular MRI: a comparison between bicuspid and tricuspid valves. European Radiology, 2019, 29, 2340-2349.	4.5	13
95	Neurological impact of emboli during adult cardiac surgery. Journal of the Neurological Sciences, 2020, 416, 117006.	0.6	13
96	An Optimized Pulse Sequence for Isotropically Weighted Diffusion Imaging. Journal of Magnetic Resonance, 1999, 140, 58-68.	2.1	12
97	Dynamic contrast-enhanced MRI parameters as biomarkers for the effect of vatalanib in patients with non-small-cell lung cancer. Future Oncology, 2014, 10, 823-833.	2.4	12
98	Effect of device inhalational resistance on the three-dimensional configuration of the upper airway. Journal of Pharmaceutical Sciences, 2005, 94, 1418-1426.	3.3	11
99	Wall motion in the stenotic carotid artery: association with greyscale plaque characteristics, the degree of stenosis and cerebrovascular symptoms. Cardiovascular Ultrasound, 2013, 11, 37.	1.6	9
100	Estimating Brain Lesion Volume Change in Multiple Sclerosis by Subtraction of Magnetic Resonance Images. Journal of Neuroimaging, 2016, 26, 395-402.	2.0	9
101	Low-contrast secondary imbibition in long rock cores. Magnetic Resonance Imaging, 1991, 9, 803-808.	1.8	8
102	Restoration of Myocardial Blood Flow Following Percutaneous Coronary Balloon Dilatation and Stent Implantation: Assessment with Qualitative and Quantitative Contrast-Enhanced Magnetic Resonance Imaging. Clinical Radiology, 2002, 57, 593-599.	1.1	8
103	Activity revealed in MRI of multiple sclerosis without contrast agent A preliminary report. Magnetic Resonance Imaging, 2000, 18, 139-142.	1.8	7
104	Application of diffusion tensor MRI to neurological segmentation. International Journal of Imaging Systems and Technology, 1999, 10, 273-286.	4.1	5
105	A Semiautomatic Method for Multiple Sclerosis Lesion Segmentation on Dual-Echo MR Imaging: Application in a Multicenter Context. American Journal of Neuroradiology, 2016, 37, 2043-2049.	2.4	5
106	Brain Tissue Pulsation in Healthy Volunteers. Ultrasound in Medicine and Biology, 2020, 46, 3268-3278.	1.5	4
107	Estimation of the Characteristic Length Scales forB0Variation Using the OE-CTPG Pulse Sequence. Journal of Magnetic Resonance Series A, 1996, 122, 222-229.	1.6	3
108	MR Image Postprocessing for Multiple Sclerosis Research. Neuroimaging Clinics of North America, 2008, 18, 637-649.	1.0	3

#	Article	IF	CITATIONS
109	Improved Assessment of Longitudinal Spinal Cord Atrophy in Multiple Sclerosis Using a <scp>Registrationâ€Based</scp> Approach: Relevance for Clinical Studies. Journal of Magnetic Resonance Imaging, 2022, 55, 1559-1568.	3.4	3
110	Measurement of dose distribution from treatment of shallow brain tumors in BNCT by NIPAM polymer gel. Progress in Nuclear Energy, 2017, 100, 292-296.	2.9	2
111	Mechanism and Clinical Significance of Precordial ST Depression in Inferior Myocardial Infarction: Evaluation by Contrast-Enhanced Dynamic Myocardial Perfusion Magnetic Resonance Imaging. Journal of Cardiovascular Magnetic Resonance, 1999, 1, 121-130.	3.3	1
112	A Semi-automatic Method for Segmentation of Multiple Sclerosis Lesions on Dual-Echo Magnetic Resonance Images. Lecture Notes in Computer Science, 2016, , 80-90.	1.3	1
113	Echoplanar MRI in patients with an acute stroke syndrome British Journal of Radiology, 1999, 72, 914-921.	2.2	0
114	Atrophy. , 2014, , 207-217.		0
115	Imaging the Effect of Anti-Angiogenic Tumor Therapy in Clinical Studies. , 2008, , 717-739.		0